Original Paper

Radiation-induced defects in CoO- and NiO-doped fluoride-phosphate glasses

Doris Möncke and Doris Ehrt

Otto-Schott-Institut für Glaschemie, Friedrich-Schiller-Universität, Jena (Germany)

Irradiation-induced defect formation is a common phenomenon in glasses. The influence of the two polyvalent ions cobalt and nickel was studied in several model glasses, two of those were fluoride-phosphate glasses. These studies were done in order to contribute to the ongoing research on solarization. Dopants and impurities may influence the intensity of intrinsic defects and may cause the evolution of additional extrinsic defects. Sample plates of high-purity glasses, undoped and doped with CoO and NiO, were irradiated by UV lamps and X-rays. The formed defect centers displayed absorption bands in the UV-VIS range, which were recorded by absorption spectroscopy. As many defect centers are paramagnetic, EPR spectra of the irradiated samples were taken.

The newly found optical bands and EPR signals evolving in the irradiated glasses are in part characteristic of intrinsic defects, which are different types of electron and hole centers connected with phosphate groups. The other signals arise from extrinsic defects, which are caused by the two dopant ions. Co^{2+} is photooxidized to $(Co^{2+})^{+}$, and replaces some of the intrinsic hole centers (POHC), while Ni^{2+} is photoreduced to $(Ni^{2+})^{-}$.

Strahlungsinduzierte Defektbildung in CoO- und NiO-dotierten Fluorid-Phosphatgläsern

Bei der Solarisation beziehungsweise der strahlungsinduzierten Defektbildung handelt es sich um ein bekanntes Phänomen, das in unterschiedlichem Maße in verschiedenen Gläsern auftritt. Um zur weiteren Aufklärung der Solarisation beizutragen, wurde, unter anderem in Fluorid-Phosphatgläsern (FP), der Einfluß der polyvalenten Ionen Cobalt und Nickel auf die Defektbildung untersucht. Dotierungen wie auch Verunreinigungen beeinflussen die Intensitäten der intrinsischen Defekte und verursachen zusätzlich die Bildung neuer Defekte. Probenplättchen hochreiner undotierter und mit CoO und NiO dotierter FP-Gläser wurden UV-Lampen und Röntgenstrahlung ausgesetzt. Da strahlungsinduzierte Defektzentren Absorptionsbanden im UV-VIS-Bereich bilden, wurde der Verlauf der Solarisation mit der optischen Absorptionsspektroskopie verfolgt. Außerdem wurden EPR-Spektren der bestrahlten Proben aufgenommen, da viele der gebildeten Defekte paramagnetisch sind.

Ein Teil der optischen Banden und EPR-Signale konnte intrinsischen Defekten zugeordnet werden, die an den Phosphatgruppen auftreten und aus unterschiedlichen Elektronen- und Lochzentren (EC und HC) bestehen. Zusätzlich treten extrinsische Defekte auf, die auf die beiden Dotierungen zurückgeführt werden können. Co^{2+} wird zu $(Co^{2+})^{+}$ photooxidiert und ersetzt als Lochzentrum einen Teil der intrinsischen POHC, andererseits wird Ni^{2+} zu $(Ni^{2+})^{-}$ photoreduziert.

1. Introduction

Radiation-induced defects in glasses deserve more attention due to the intensified applications of stronger lamps and lasers, working at increasingly shorter wavelengths. Solarization describes the effect of decreased transmission in the UV and VIS due to color centers generated by irradiation. These color centers, or defects, evolve when the irradiated light suffices to ionize the glass and they consist of electron centers (EC) and hole centers (HC) [1]. Defects can further be divided in intrinsic defects, which arise from the glass matrix itself, and extrinsic defects, which are caused by dopants or impurities.

Received 30 August 2000, revised manuscript 15 December 2000.

Cobalt- and nickel-doped glasses are used as optical filters. They show high transmission from 250 to 400 nm. At the same time the absorption between 450 and 700 nm is very strong. Cobalt and nickel are polyvalent as well as polycoordinated ions. These ions are hardly ever seen in glasses in any other oxidation state than +2. In this state, the coordination is either tetrahedral (T_d) or octahedral (O_h), strongly depending upon the glass matrix. The differently coordinated ions show distinctive spectra and subsequently colors, leading to their use as structure indicators [2].

The optical basicity (Λ) of the glass is a measure of the electron donor power of the glass matrix [3 to 6]. Λ is proportional to the electron density on the oxide and can be correlated to the coordination of Co^{2+} and Ni^{2+} [7]. In more acidic glasses the ions show ionic-bonded

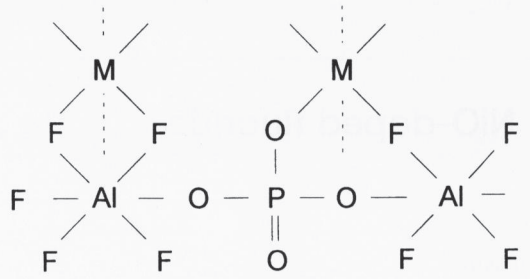

Figure 1. Schemata of the structural model of fluoride-phosphate glasses (fluoroaluminate-type) [8].

octahedral coordination, while covalent-bonded tetrahedral coordination prevails in high-basicity glasses.

Fluoride melts of the fluoroaluminate type are atypical glass forming systems. Their strong ionic bonding character results in very low melting viscosities ($\eta \approx 10^{-2}$ dPa s, at melting temperatures of $\vartheta \approx 1000\,°C$). This viscosity is comparable to that of water at room temperature. Doping small amounts of phosphates drastically increases the glass forming abilities of the melts which have otherwise a great tendency to devitrify during cooling. The structure model of fluoride-phosphate glass (FP) can be described as chains of $Al(F,O)_6-O_h$ bonded with mono- and diphosphate groups and cations (figure 1). It was found by Raman and NMR spectroscopy that mono-phosphate groups dominate in FP4 and diphosphates in FP20 glass types [8]. FP glasses have been commercially melted and, due to their special optical properties, are attractive candidates for application in high-performance optics and laser technology [9]. The intrinsic absorption in the UV region arises from electron transitions in the band gap. Fluoroaluminate glasses with low phosphate contents have a wide band gap, which is comparable to that of pure silica glass or the fluoride single crystal CaF_2. The band gap becomes smaller with increasing phosphate content [1].

The effect of different radiation sources was investigated in several model glasses. The glasses range from the acidic fluoride-phosphates over phosphates to high-basicity (boro-)silicates (table 1). Hardly any solarization is seen in the more acidic glasses, especially when relative weak lamp irradiation is applied. Of all the studied glasses, only the phosphate glass shows significant intrinsic defects. In comparison, the undoped (boro-)silicate glasses are quite stable against solarization. However, the (boro-)silicate glasses doped with Co^{2+} and Ni^{2+} in tetrahedral coordination give very strong effects [10]. These extrinsic defects could be ascribed to the photooxidation of Co^{2+} and Ni^{2+} forming $(Co^{2+})^+$ and $(Ni^{2+})^+$ [11].The high-basicity glass matrix stabilizes the higher oxidation states in these glasses.

Phosphate-bonded defects are more stable than F-bonded defects. Therefore, radiation-induced defects formed in FP glasses are connected primarily to phosphate sites. The kinetics of formation and recovery of the radiation-induced defects in FP glasses irradiated with lamps and lasers have been intensively studied. The numerous induced intrinsic defects were characterized by EPR and optical spectroscopy [12 to 14]. Based on these former results on solarization in undoped glasses, the aim of this work is to investigate in two FP glasses the influence of the dopants NiO and CoO on the characterized defects and the formation of any new defect centers.

2. Experimental procedures

Table 1 states the compositions and some characteristic data of several model glasses studied. The FP glasses were melted in an electric furnace at 1000 °C, in Pt-crucibles with educts to yield 100 g glass. They were cooled in graphite molds from 500 °C to room temperature with a cooling rate of about 30 K/h. Additionally these glasses were melted under reducing conditions. 30 g charges were remelted in carbon crucibles in a graphite furnace under a flowing argon atmosphere. Table 1 states, for comparison, the compositions and optical basicities of other model glasses studied. The phosphate glasses were melted at 1350 °C in SiO_2 crucibles. The glasses were melted as undoped base glasses, further doped with 0.3 mol% CoO or NiO, respectively, and also with 0.15 mol% both CoO and NiO. Only high-purity reagents were used for melting, so that the iron content of the glasses is as low as 5 to 10 ppm.

Polished samples, 1 and 2 mm thick, were irradiated with high-pressure mercury lamps and X-rays. Of the two lamps utilized one was an HOK lamp, the other one a weaker 1 kW HgXe broad band lamp, working in a sun simulator from ORIEL. Table 2 states the parameters of the irradiation sources. Irradiation by lamp lasted up to 100 h to ensure that the defect formation reached a saturation level. For X-rays the irradiation lasted 16 h. The lamps continuously emit a wide spectrum from the UV to NIR. The spectral power density of both lamps was about 1500 W/m^2 below 280 nm. This part of the spectrum causes most of the solarization damage. The XeHg lamp works at slightly higher wavelengths (> 230 nm) than the HOK lamp (> 190 nm) and thus gives rise to less solarization. Irradiation by the HOK lamp was applied by SCHOTT GLAS in Mainz (Germany). For X-ray irradiation the sample plates were subjected to a Cu cathode radiation of 10 kW at a distance of 80 cm. For all samples the optical spectra were taken right after the irradiation process. And all, but the samples irradiated with the HOK lamp, were analyzed by EPR spectroscopy within the next days. As the samples show a rapid defect recovery and the defects are very small, no significant EPR signals could be observed in the glasses irradiated with the HOK lamp when analyzed later at the university of Jena.

Table 1. Composition (in mol%) and characteristics of the model glasses studied

	FP4	FP20	P100	NBS2	NCS	NBS1
	4 $Sr(PO_3)_2$ 96 {AlF_3, MgF_2, SrF_2, CaF_2}	20 $Sr(PO_3)_2$ 80 {AlF_3, MgF_2, SrF_2, CaF_2}	100 $Sr(PO_3)_2$	74 SiO_2 21 B_2O_3 4 Na_2O 1 Al_2O_3	74 SiO_2 10 CaO 16 Na_2O	74 SiO_2 10 B_2O_3 16 Na_2O
Λ_{th} (Λ_{Pb})[1]	0.35 (0.34)	0.38 (0.48)	0.46 (0.47)	0.48	0.579	0.53
ΣFe in ppm	10	10	8	5	5	6
Fe^{3+} in ppm	6	6	5			
T_g in °C	440	480	515	442	532	553
n_e	1.43	1.50	1.56	1.47	1.52	1.51
ϱ in g/cm³	3.46	3.51	3.15	2.18	2.48	2.45
coordination	O_h	O_h	O_h	O_h	T_d	T_d
color[2] {Co	violet	violet	violet	violet	blue	blue
color[2] {Ni	amber	amber	amber	yellow-green	brown	violet
solarization	less pronounced	less pronounced	less pronounced	less pronounced	very strong	very strong

[1] Medium theoretical optical basicity values according to Duffy [3 to 6], in brackets experimental values for the Pb^{2+} indicator ion as found by Seeber [25].
[2] NiO or CoO were doped in concentrations of 0.3 mol%, respectively.

Table 2. Irradiation sources

source	range	spectral performance		irradiation time in h
XeHg lamp	UV-NIR	I: 1500 W/m²	λ: 230 to 280 nm	up to 100
HOK lamp	UV-NIR	I: 1500 W/m²	λ: 190 to 280 nm	up to 100
X-ray		Cu cathode: 10 kW (50 kV, 200 mA)		up to 16

Note:
I = spectral power density,
λ = wavelength of the band maximum (error ± 5 nm).

UV-VIS-NIR spectra were used to characterize the glasses and to observe the development of irradiation-induced defects. A double beam spectrophotometer (UV-3102, Shimadzu) was employed, recording the extinction $E = \lg(I_0/I)$ (error < 1 %), which was later standardized to a nominal path length (d) of 1 cm. The induced extinction, or change of optical density, $\Delta E/d$, caused by the irradiation is used to describe the intensity of the defects formed. The bands of the evolving electron centers are usually found near the UV edge. In this range the dopants absorb strongly too, complicating the evaluation of the optical bands. Therefore, a second independent analytical method, the Electron Paramagnetic Resonance spectroscopy (EPR), was applied. For better comparison the glasses were also analyzed with the addition of the spin standard dpph (1,1-diphenyl-2-piterylhydrozyl). Although Co^{2+} and Ni^{2+} compounds are known to be successfully investigated by EPR, Co^{2+} and Ni^{2+} in glass give no significant EPR signals and could only be detected at extremely low temperatures [15]. EPR spectroscopy permits the detection of paramagnetic EC and HC in the glasses at room temperature without interferences from the two dopants [10]. The EPR spectrometer used (ESP 300 E, Bruker), worked with a frequency band of $\nu \approx 9.78$ GHz at room temperature. Band separation of the spectra was accomplished on the computer with customary auxiliary software. The resolved Gaussian bands were correlated with the defect centers detected by EPR and thermal recovery measurements.

3. Results and discussion

Co^{2+} and Ni^{2+} in FP glasses are octahedrally coordinated. The optical spectra of the glasses can be seen in figures 2a and b. Absorption of the CoO-doped glasses is smaller for the more acidic FP4 than for the FP20. As no differences were observed in NiO-doped glasses, this change of absorption might be caused by a slightly higher T_d content in the case of Co^{2+}. Because of different symmetries (presence/absence of an inversion center) the molar extinction coefficient is about 100 times higher for T_d than for O_h coordination [16]. The two ions have different energetic preferences for the different coordinations. Ni^{2+} strongly favors the O_h form over T_d, but Co^{2+} shows no such distinction. The shoulder at 250 nm is caused by the charge-transfer (CT) transition of Fe^{3+},

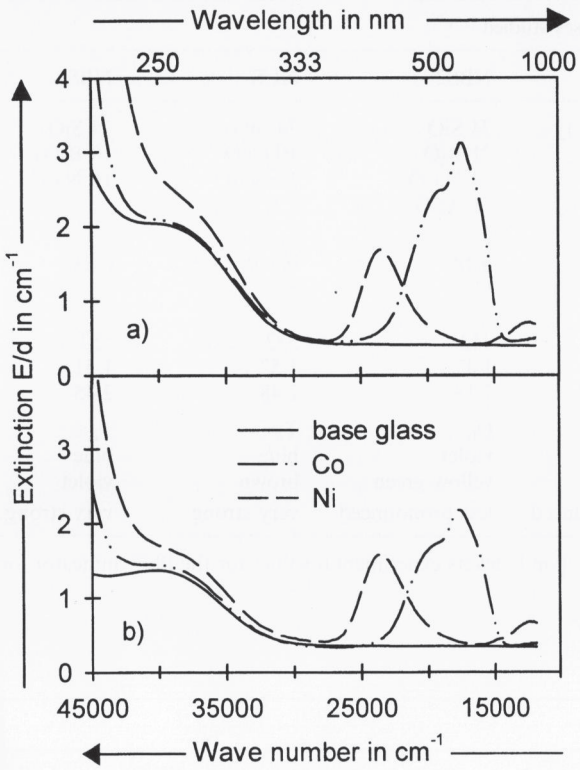

Figures 2a and b. Optical spectra of the preirradiated FP glasses, a) FP20, b) FP4. Undoped base glass (——), doped with CoO (··—··—), doped with NiO (– – –).

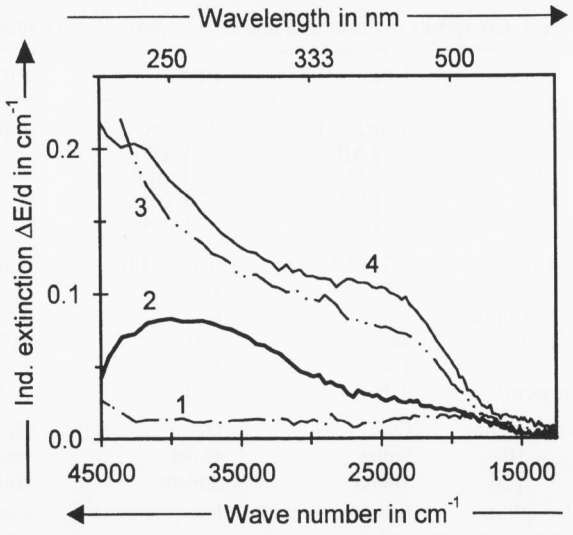

Figure 3. Induced optical spectra of FP20 glasses after 100 h XeHg lamp irradiation; curve 1: undoped base glass, curve 2: doped with NiO, curve 3: doped with CoO and NiO, curve 4: doped with CoO.

while the absorption edge is dominated by the CT transition of the dopants.

Two general observations could be made regarding the solarization observed in the glasses. The main difference in the induced optical spectra of the normal- and the reduced-melted glasses is due to the photooxidation of Fe^{2+} to $(Fe^{2+})^{+}$. A strong absorption at 250 nm arises from the CT transition of the oxidized iron (see in detail Ehrt et al. [8]). Next to the photooxidation of iron hardly any changes in the solarization were found when normal- and reduced-melted glasses containing the same dopant were compared. This was expected, as the different melting conditions do not influence the oxidation state of cobalt or nickel, nor their coordination. Solarization in glasses simultaneously doped with CoO an NiO can be explained by the combination of the defects found in each of the monodoped glasses. Further discussion will therefore concentrate on the undoped and monodoped glasses melted under normal conditions.

3.1 Radiation by lamp

No induced defects were observed after XeHg lamp irradiation of the undoped FP glasses melted under normal conditions. FP glasses are extremely resistant, while pure phosphate glasses are easily solarized by UV lamp irradiation. This solarization is due to the formation of intrinsic EC and HC in the network. The weak lamp irradiation does not lead to significant solarization in the FP4 glasses, although a weak increase of absorption might be observed for the doped glasses. The latter is more pronounced when the stronger HOK lamp is applied, but further evaluation would hardly exceed the error margins. Solarization is stronger in the FP20 system. This can be expected, as phosphate-bonded defects seem to be more stable than F-bonded, and FP20 offers more phosphate sites than does FP4. Irradiation with the XeHg lamp leads, especially in the CoO-doped FP20, to notable defects (figure 3). As the signal-noise ratio is still very bad, no band separation was attempted. Defects in the HOK lamp irradiated FP20 samples are at least twice the magnitude of those in samples irradiated by the weaker lamp. Form and magnitude of these undoped base glass defects resemble the known intrinsic defects in FP glasses and have been characterized by optical and EPR spectroscopy (table 3). Figures 4a to c show the band separation for the defects of the FP20 glasses based on parameters for undoped glass according to Ebeling [12 and 13]. The three bands of the phosphate-bonded HC (POHC) lie at longer wavelengths; those of the corresponding EC near the UV.

The intensity of the bands of the defects in the NiO-doped glass is of the same magnitude as in the base glass. Band separation shows that the magnitude of the POHC band is comparable with the band in the undoped glass, though the band of the oxygen-attached OHC is increased by a factor of three. The intensity of the PO_4EC band is increased by a factor of two. This band and the other bands of EC at shorter wavelengths are overlapped by the UV edge of the colored glasses,

Table 3. Paramagnetic constants and optical absorption of radiation-induced defects in phosphate glasses based on Ebeling [12 and 13]

defect type	EPR parameters[3]	optical absorption[4]		
		λ in nm	E′ in eV	W′ in eV
POHC	$W = 1$ mT $A_{iso} = (4.0 \pm 0.3)$ mT $g_m = 2.008 \pm 0.003$	540 430 325	2.30 ± 0.02 2.89 ± 0.04 3.82 ± 0.04	0.50 1.00 1.12
PO_3EC	$W = 10$ mT $A_{iso} = (86 \pm 2)$ mT $g_m = 2.064 \pm 0.005$	210	5.90 ± 0.06	1.00
PO_4EC	$W = 9$ mT $A_{iso} = (126 \pm 2)$ mT $g_m = 2.142 \pm 0.008$	240	5.12 ± 0.06	1.00
PO_2EC[5]	$W = 7$ mT $A_{iso} = (27 \pm 2)$ mT $g_m = 2.006 \pm 0.003$	265	4.68 ± 0.08	1.00
OHC[6]	$W = 7$ mT $g = 2.014 \pm 0.001$	290	4.28 ± 0.06	1.00
$(Co^{2+})^+HC$[7]	no signal	300 450	4.13 ± 0.01 2.75 ± 0.03	1.24 1.20
$(Ni^{2+})^-EC$[7]	$W_1 = 18$ mT $g_1 = 2.26$ $W_2 = 9$ mT $g_2 = 2.10$	350	3.54 ± 0.03	1.00

[3] W = half amplitude width of the line; $A_{(iso)}$ = (isotrope) hyperfine splitting due to ^{31}P, the distance (in mT) between two lines; g_m = the middle value between g values of both lines of a doublet: $g_{mid} = (g_1 + g_2)/2$.
[4] λ = wavelength of the band maximum (error ± 5 nm); E' = energy of the band maximum; W' = half amplitude width of the band (error ± (0.03 to 0.07) eV).
[5] Form and evolution of this center are not yet satisfactorily explained.
[6] Oxygen-related center of unknown structure.
[7] Parameters of the extrinsic defects observed in this study.

making further evaluation difficult. The fit of the optical spectra needs an additional band at 350 nm, a band correlated in the literature with Ni^+ [17].

For cobalt, the spectra are more distinct. The magnitude of the defects is about ten times as high as in the other glasses. For the fit no bands of intrinsic HC such as POHC or OHC were needed: only two new bands at 300 and 450 nm. The optical spectra of octahedral Co^{3+} is described in the additional literature with two bands between 300 and 500 nm [18]. The formed $(Co^{2+})^+$ replaces the POHC and the additional increase of HC is covered by a subsequent increase of the known EC, sited at the glass matrix.

The EPR spectra (not shown) are not very different from those of unirradiated samples as most of the centers have already recovered by the time of analysis, only hints of the POHC signals are found in the undoped and NiO-doped glasses. No POHC signals were found for CoO-doped glasses and thus even these slim results agree well with the interpretation of the optical spectra.

Photooxidation of Co^{2+} has been established before in high-basicity glasses, where the CT transition of T_d $(Co^{2+})^+$ dominates the optical spectra [10]. Photoreduction of polyvalent ions, though less common, has for example been observed in silicate glasses for iron [19]. Nickel has a lower redox potential than cobalt, and the acidic glasses do not stabilize the oxidized form in the way the silicates do. This might explain why NiO-doped glass shows the opposite effect of CoO-doped glass.

3.2 Radiation by X-rays

UV irradiation has been compared to striking one key of a piano and X-ray irradiation to the fall of the same piano down a staircase [20]. The high-energy X-ray irradiation will excite all kinds of possible effects, while lamp irradiation excites only a well defined number of defects. Therefore, extrapolation from X-ray to long-term UV-lamp solarization is not advisable. The results

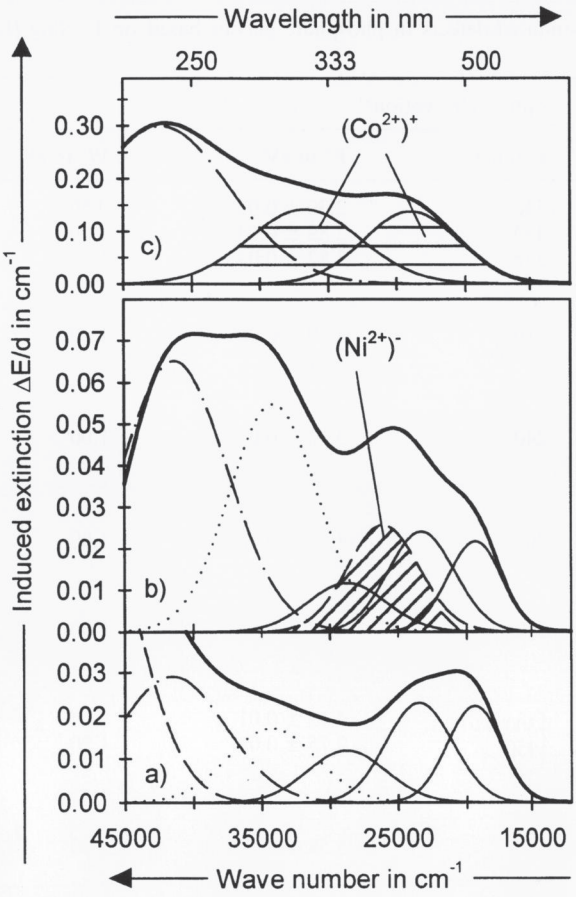

Figures 4a to c. Induced optical spectra including band simulation of FP20 after 100 h HOK lamp irradiation; a) undoped base glass, b) NiO-doped and c) CoO-doped. POHC (——), OHC (·····), PO_2EC (·—·—), PO_4EC (— — —), $(Co^{2+})^+$ HC (═══), $(Ni^{2+})^-$ EC (////).

of the X-ray irradiation should be discussed nevertheless, as only this method gave significant defects for both FP glasses.

When X-ray irradiation is studied the magnitude of the defects is for both glasses far beyond the error margins. Figure 5 displays the induced optical spectra of the strong solarization in the FP glasses. The EPR spectra are as intense and show a strong resemblance for the differently doped and undoped glasses (figures 7 and 8). Figure 6 gives an example for the characteristic form of the EPR signals found in undoped phosphate glasses and states also the parameters attributed to the different defects according to Ebeling [12]. The high similarity with the spectra of the fluoride-phosphate glasses illustrates the fundamental role of phosphate groups in the defect formation of FP glasses.

The EPR spectra show for CoO-doped glasses a sharp decline of the POHC and a small increase in the EC signals. The optical spectra for the CoO-doped glass can as before be fitted by adding two new bands at 300 and 450 nm and reduced POHC bands. The intensity of the X-ray induced $(Co^{2+})^+$ bands is about 40 times higher than after HOK lamp irradiation.

The EPR spectra of the NiO-doped glasses show that the POHC concentration remains constant, but the EC decrease slightly. Additionally two new signals are found on the higher g side between $g \approx 2.0$ and 2.4. These signals are superimposed on the known intrinsic EC signals and are also found in the glasses doped with CoO and NiO. The signals of the $(Ni^{2+})^-$EC is weaker for the glasses doped with both ions which contain only 0.15 mol% NiO.

The fit of the optical spectra as before includes the additional band at 350 nm. This band is smaller in the glasses doped with both ions than in those only doped with NiO. Compared to the other glasses the intensity of the OHC band is significantly higher for the NiO-doped glasses. The experimental optical data thus supports the reading as photoreduction of Ni^{2+} to $(Ni^{2+})^-$.

Even though Co^{2+} and Ni^{2+} in glasses do not display a signal in the EPR spectra at room temperature, Ni^+ as d^9, or inverse d^1, species seems to exhibit its own signal. However, the EPR data on Ni^+ in the literature is not as easily applicable to glasses as the optical data. Generally signals connected to Ni^+ were found on the low field side with g values between 2.0 to 2.5 [21 to 23]. The g values exhibit anisotropicity depending on the ligands, the coordination of nickel, the temperature of the measurement, or the orientation of the crystal if the ion is embedded in one. Glasses are normally isotropic and this leads, together with different degrees of distortion within the glass, to a broadening of the signals. This wide structural range causes a broadening of the signal and might be one reason why, at room temperature, Co^{2+} and Ni^{2+} show no visible signals in glasses [15, 22 and 23]. Another explanation for the absence of a Co^{2+} and Ni^{2+} signal might arise from a tetragonal or trigonal distortion of their complexes, leading to low-lying excited states instead of the normally found degeneracy of octahedral complexes. The low-lying excited state results from minimal quenching of orbital motion and gives rise to exceedingly short relaxation times and large spectral anisotropies. The latter causes the particularly smear out of the spectra observed in glasses, while the short relaxation times lead to the enormous line widths at practical laboratory temperatures [24]. (When preirradiated CoO-doped model glasses were analyzed at temperatures between 4 and 77 K, a broad signal was found at g values between 4 and 7.)

Most spectra of Ni^+ in the literature at least have two strong unsymmetrical signals in common, which are centered around $g \approx 2.0$ (±0.1) and $g \approx 2.3$ (±0.2). The signals found in the NiO-doped FP glasses at $g = 2.26$ superimposed on the PO_4EC signal and at $g = 2.10$ pinned between the PO_3EC, and the POHC signal agree well with the literature data of Ni^+, considering the different analytical circumstances. It was surprising that in this study the Ni^+ signal can be found at room tempera-

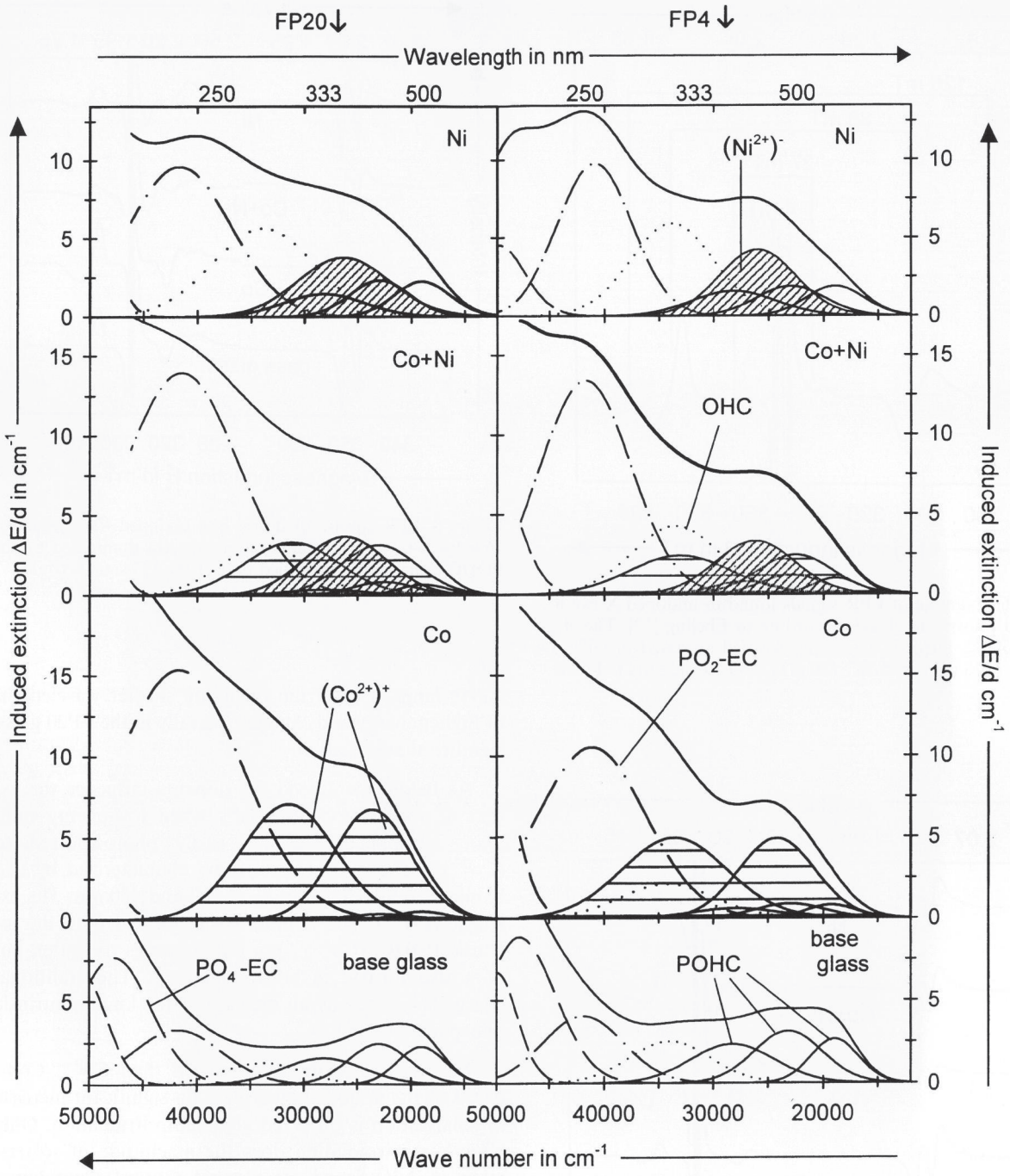

Figure 5. Induced optical spectra including band simulation of X-ray irradiated doped and undoped FP20 (left) and FP4 (right). Representative bands of typical induced defects have been specially labeled; POHC (——), OHC (·····), PO_2EC (·—·—), PO_4EC (— —), PO_3EC (– – –), $(Co^{2+})^+$ HC (═══), $(Ni^{2+})^-$ EC (////).

ture, although compounds analyzed in the references only display a signal when the spectra were taken below 160 K. One explanation might be a longer life time of the $(Ni^{2+})^-$ spezies in the acidic FP glasses compared to the frozen organometallic complexes or crystals described in the literature. Together with the results of the optical spectroscopy the EPR data confirm that the influence of Ni^{2+} on the solarization in FP glasses is due to the photoreduction of Ni^{2+} to $(Ni^{2+})^-$.

4. Conclusion

Solarization is influenced mostly by the chosen irradiation source. As expected, the high-energy X-rays induce intense and distinct defects. The magnitude of these defects is at least 100 times higher than after lamp irradiation. While solarization by X-rays is of similar magnitude for all undoped and doped glasses, lamp irradiation results in transmission losses which highly

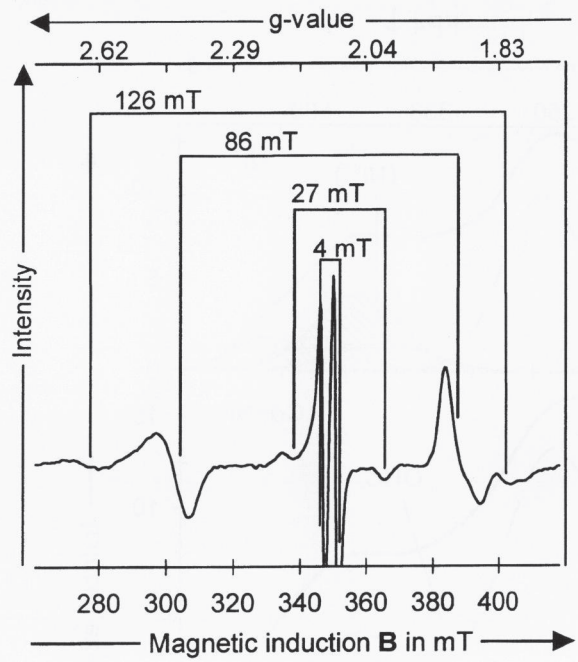

Figure 6. Example of EPR signals found in undoped X-ray irradiated phosphate glasses according to Ebeling [12]. The A_{iso} values of the intrinsic defects are labeled as stated in table 3: PO_4EC (126 mT), PO_3EC (86 mT), PO_2EC (27 mT), POHC (4 mT).

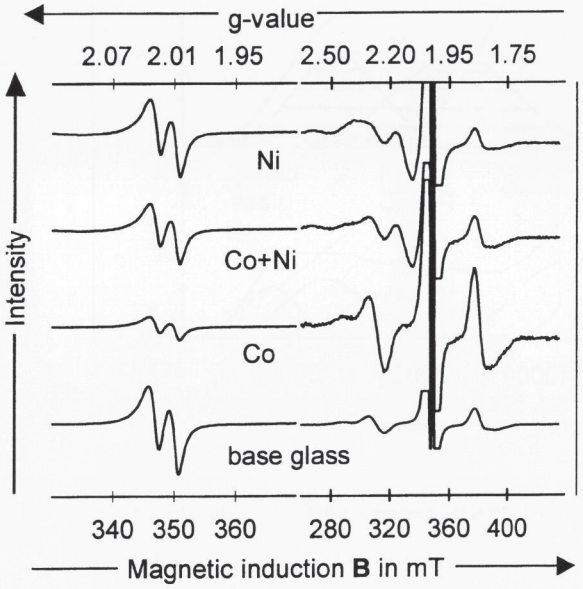

Figure 7. EPR spectra of doped and undoped FP20 irradiated 16 h by X-rays, dpph-standardized: spectra dominated by the POHC signal (left), magnified part of the EC signals (right).

depend on the glass matrix and the dopants. The XeHg lamp hardly leads to any defects. Weak defects are found only in CoO-doped glasses, they do not exceed the error margins. The HOK lamp emits, when compared to the

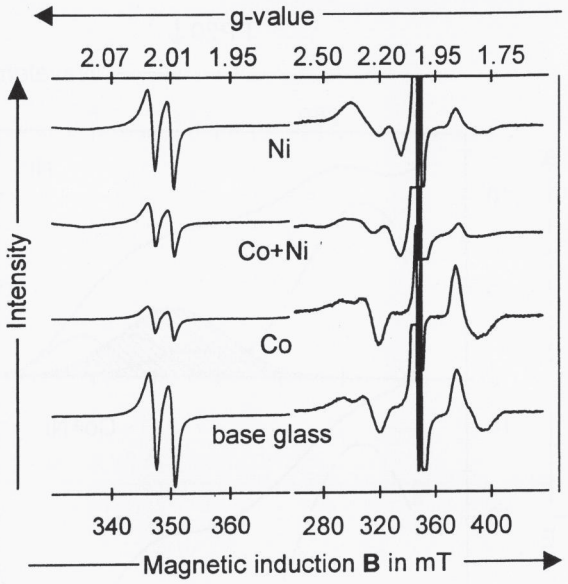

Figure 8. EPR spectra of doped and undoped FP4 irradiated 16 h by X-rays, dpph-standardized: spectra dominated by the POHC signal (left), magnified part of the EC signals (right).

XeHg lamp, a spectrum including shorter wavelengths of higher energy and causes, especially in the FP20 glass, significant solarization.

As before mentioned the dopants influence the extent of solarization, especially when low-energy radiation is applied. Co^{2+} is easily photooxidized to $(Co^{2+})^+$. The optical spectra are characterized by two bands of similar magnitude at 300 and 450 nm. The extrinsic $(Co^{2+})^+$ HC is more easily formed than the intrinsic POHC. $(Co^{2+})^+$ not only replaces the latter, but it is also formed in greater numbers. The additional charge is covered by an increase of the known intrinsic phosphate-bonded EC.

Ni^{2+} is less easily photoionized than Co^{2+}. Compared to the undoped base glass no significant increase of solarization is observed after lamp irradiation. Only after X-ray irradiation does the magnitude of solarization in NiO-doped glass equal that of CoO-doped glasses. In contrast to Co^{2+}, Ni^{2+} is photoreduced to $(Ni^{2+})^-$. The optical spectra show an additional band at 350 nm, which compares well with the literature data of Ni^+. The EPR spectra also reveal additional signals at $g = 2.26$ and $g = 2.10$. Although Co^{2+} and Ni^{2+} show no visible EPR signals at room temperature in glass, Ni^+ as d^9, or inverse d^1, species displays its own signals.

Phosphate-bonded defects are assumed to be more stable than F-bonded defects. As expected, FP20 with its higher phosphate content is more prone to solarization than FP4. After lamp irradiation only the CoO-doped glasses show significant defects. These defects were more pronounced in FP20 than in FP4. The cobalt-connected defects arise from photooxidation to $(Co^{2+})^+$,

and, as expected, evolve more defects in the less acidic FP20 than in FP4.

The magnitude of solarization after X-ray irradiation was similar for both glasses and both dopants. However, small differences can be seen, especially in the glasses simultaneously doped with CoO and NiO. Comparison of the $(Ni^{2+})^-/(Co^{2+})^+$ ratios of the two glasses shows that the formation of the photoreduced species is favored by the acidic glass matrix and that of the photooxidized species is notably enhanced by the less acidic FP20 glass matrix.

5. References

[1] Ehrt, D.; Seeber, W.: Glass for high performance optics and laser technology. J. Non-Cryst. Sol. **129** (1991) p. 19–30.

[2] Weyl, W.: Coloured Glasses. Sheffield: Soc. Glass Technol., 1951. p. 168.

[3] Duffy, J. A.: A common optical basicity scale for oxide and fluoride glasses. J. Non-Cryst. Solids. **109** (1989) p. 35–39.

[4] Baucke, F. G. K.; Duffy, J. A.: Oxidation states of metal ions in glass melts. Phys. Chem. Glasses. **35** (1994) no. 1, p. 17–21.

[5] Duffy, J. A.: Redox equilibria in glass. J. Non-Cryst. Solids. **196** (1996) p. 45–50.

[6] Duffy, J. A.: Charge transfer spectra of metal ions in glass. Phys. Chem. Glasses. **38** (1997) no. 6, p. 289–292.

[7] Paul, A.; Douglas, R. W.: Optical absorption of divalent cobalt in binary alkali borate glasses and its relation to the basicity of glass. Phys. Chem. Glasses. **9** (1968) no. 1, p. 21–26.

[8] Ehrt, D.; Natura, U.; Ebeling, P. et al.: Formation and healing of UV radiation defects in phosphate and fluoride phosphate glasses with high UV transmission. In: Choudhary, M. K.; Huff, N. T.; Drummond III. C. H. (eds.): Proc. XVIII International Congress on Glass. San Francisco, CA (USA) 1998. Westerville, OH (USA): The Am. Ceram. Soc., 1998. Session C10, p. 1–6. Only published on CD-ROM.

[9] Ehrt, D.; Leister, M.; Matthai, A.: Redox Behaviour in Glass Forming Melts. Molten Salt Forum **5-6** (1998) p. 547–554.

[10] Möncke, D.; Ehrt, D.: Radiation defects in CoO and NiO doped glasses of different structure. In: Proc. 5th Conf. European Society of Glass Science and Technology (ESG), Prague 1999. Vol. B4, p. 49–56. (Available on CD-Rom from Czech Glass Society.)

[11] Natura, U.; Ehrt, D.: Formation of radiation defects in silicate and borosilicate glasses caused by UV lamp and excimer laser radiation. Glastech. Ber. Glass Sci. Technol. **72** (1999) no. 9, p. 295–301.

[12] Ebeling P.: Strahlungsinduzierte Defekte in Phosphatgläsern. Universität Jena, PhD. thesis 2000.

[13] Ehrt, D.; Ebeling, P.; Natura, U.: UV Transmission and radiation-induced defects in phosphate and fluoride-phosphate glasses. J. Non-Cryst. Solids. **263 & 264** (2000) p. 240–250.

[14] Ebeling, P.; Ehrt, D.; Friedrich, M.: Study of radiation-induced defects in fluoride-phosphate glasses by means of optical absorption and EPR spectroscopy. Glastech. Ber. Glass Sci. Technol. **73** (2000) no. 5, p. 156–162.

[15] Gan, F.; Deng, H.; Liu, H.:Paramagnetic resonance study on transition metal ions in phosphate, fluorophosphate and fluoride glasses, Part 2: Co^{2+} and Ni^{2+}. J. Non-Cryst. Sol. **52** (1982), p. 143–149.

[16] Bates, T.: Ligand field theory and absorption spectra of transition-metal ions in glasses. In: Mackenzie, J. D. (ed.): Modern aspects of the vitreous state. Vol. 2. London: Butterworths, 1962. p. 195–254.

[17] Buxton, G. V.; Sellers, R. M.: Pulse radiolysis study of M^+ ions. J. Chem. Soc. Faraday Trans. **7** (1975) p. 558–567.

[18] Linard, M.; Weigel, M.: Lichtabsorption von Mono- und Diacido-amminen des dreiwertigen Kobalts mit Fettsäureresten. Z. anorg. Allg. Chem. **264** (1951) p. 321–335.

[19] Nofz, M.; Reich, C.; Stösser, R. et al.: On the interaction of glasses with high-energy radiation – Combined ESR and optical studies. Glastech. Ber. Glass Sci. Technol. **72** (1999) no. 3, p. 76–90.

[20] Blasse, G.; Grabmair, B. C.: Luminescent materials. Berlin et al.: Springer, 1994. p. 11.

[21] Pilbrow, J. R.: Transition ion electron paramagnetic resonance. Oxford: Clarendon, 1990. p. 327–331.

[22] Van Robroeck, L.; Goovaerts, E.; Shoemaeker, D.: Electron-spin-resonance study of Co^{2+} and Ni^+ centers in AgCl (Cu, Co, Ni). Phys. Stat. Sol. (b) **132** (1985) p. 179–187.

[23] Sreeramachandra Prasad, L.; Subramanian, S.: E.P.R. of Ni(I) radiolytically produced in Ni(II)doped Cd(imidazole)$_3SO_4H_2O$. Mol. Phys. **57** (1986) no. 3, p. 543–552.

[24] Griscom D. L.: Electron spin resonance in glasses. J. Non-Cryst. Sol. **40** (1980) p. 211–272.

[25] Seeber, W.: Kombination experimenteller und theoretischer Methoden der Absorptions- und Lumineszenzspektroskopie zur Entwicklung amorpher Materialien für Optik und Optoelektronik – Am Beispiel von Fluoridphosphatgläsern. Universität Jena, habilitation thesis 1995.

0301P003

Address of the authors:

D. Möncke, D. Ehrt
Otto-Schott-Institut für Glaschemie
Friedrich-Schiller-Universität Jena
Fraunhofer Straße 6
D-07743 Jena